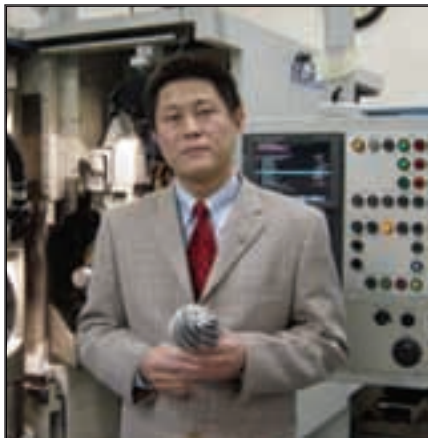
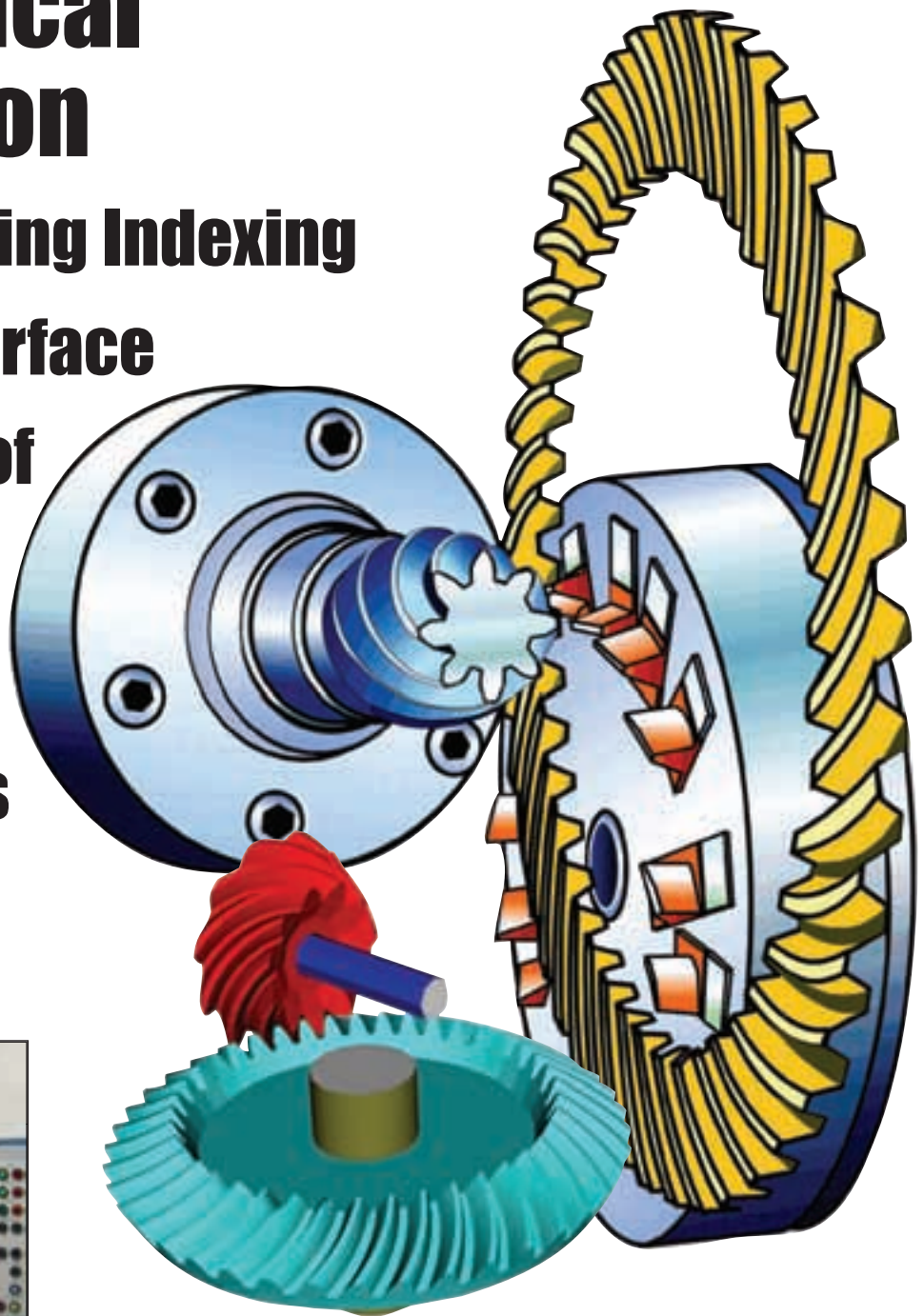


Kinematical Simulation of Face Hobbing Indexing and Tooth Surface Generation of Spiral Bevel and Hypoid Gears

Dr. Qi Fan



Dr. Qi Fan is a bevel gear theoretician at The Gleason Works of Rochester, NY. Prior to that, he worked in the Gear Research Center at the Mechanical and Industrial Engineering Department at the University of Illinois at Chicago. Fan has authored more than 20 papers on bevel gear research.



Management Summary

In addition to the face milling system, the face hobbing process has been developed and widely employed by the gear industry for manufacturing spiral bevel and hypoid gears. However, the mechanism of the face hobbing process is not well known by gear researchers and engineers. This paper presents the generalized theory of the face hobbing process, mathematical models of tooth lengthwise curve generation and tooth surface generation. The face hobbing indexing motion is simulated and visualized. A face hobbing tooth surface generation model is developed, which is directly related to the kinematical mechanisms of a physical bevel gear generator. The developed mathematical models accommodate two categories of the face hobbing system: non-generating (Formate) and generating.

Introduction

There are two types of face hobbing processes used to generate the tooth surfaces of spiral bevel and hypoid gears, a non-generated (Formate®) process and a generated process (Refs. 1, 2, 3). However, the pinion is always manufactured using a generated process.

The major differences between the face milling process and the face hobbing process are: (1) in the face hobbing process, a timed continuous indexing is provided, while in the face milling process, the indexing is intermittently provided after cutting each tooth side or slot. Similar to the face milling process, in the face hobbing process, the pinion is cut with a generated method and the gear can be cut with either a non-generated (Formate®) or a generated method. The Formate method offers higher productivity than the generating method because generating roll is not applied in the Formate method. However, the generating method offers more freedom for controlling tooth surface geometries; (2) the lengthwise tooth curve of face milled bevel gears is a circular arc, while that of face hobbed gears is an extended epicycloid; and (3) face hobbing gear designs use a uniform tooth depth system, while face milling gear designs use a tapered tooth depth system.

Theoretically, the face hobbing process is based on the generalized concept of bevel gear generation in which the mating gear and the pinion can be considered respectively generated by the complementary generating crown gears, as shown in Figure 1. The tooth surfaces of the generating crown gear are kinematically formed by the traces of the cutting edges of the tool blades, as shown in Figure 2. The generating crown gear can be considered as a special case of a bevel gear with 90° pitch angle. Therefore, a generic term “generating gear” is usually used. The concept of a complementary generating crown gear is considered when the generated mating tooth surfaces of the pinion and the gear are conjugate. In practice, in order to introduce mismatch and crowning of the mating tooth surfaces, generating gears for the pinion and the gear may not be complementarily identical. The rotation of the generating gear is represented by the rotation of the cradle on a hypoid gear generator.

The face hobbing system can use advanced design methodology to formulate the parameters of the generating gears. As a

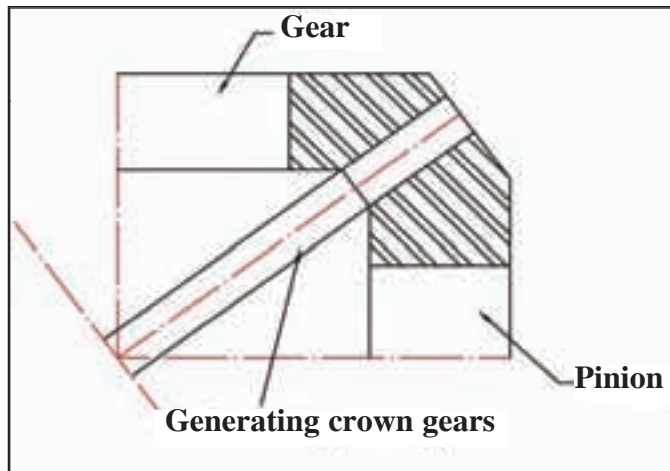


Figure 1—Basic concept of bevel gear generation.

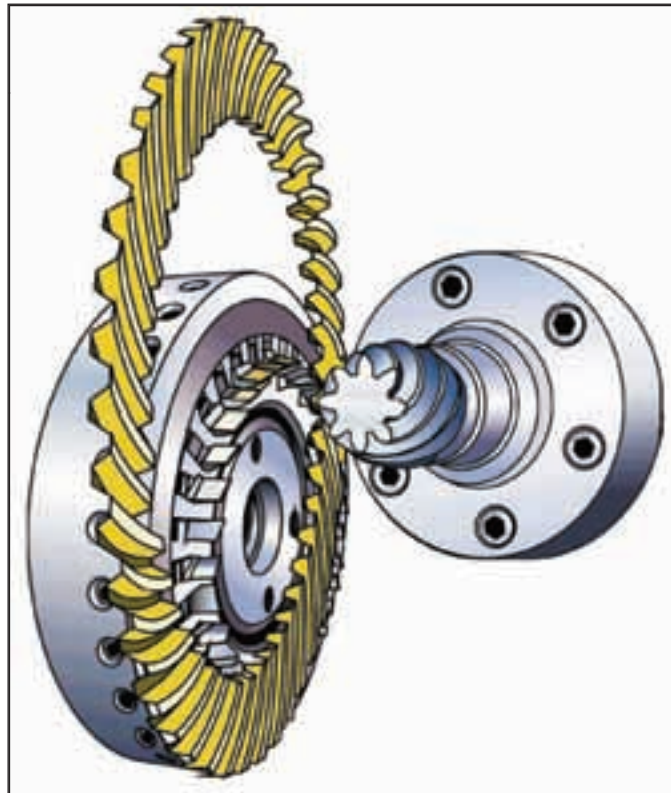


Figure 2—Relationship of the cutting tool, generating gear and the work.

result, face hobbed spiral bevel and hypoid gear sets can offer optimized bearing contact, bias direction and function of transmission errors, resulting in reduced working stresses, vibration and noise. Optimized face hobbed gear sets are less sensitive to errors of alignment.

Related Motions of the Face

Hobbing Process

In the generated face hobbing method, two sets of related motions are defined. The first set of related motions is the rotation of the tool (cutter head) and the rotation of the work (workpiece), namely,

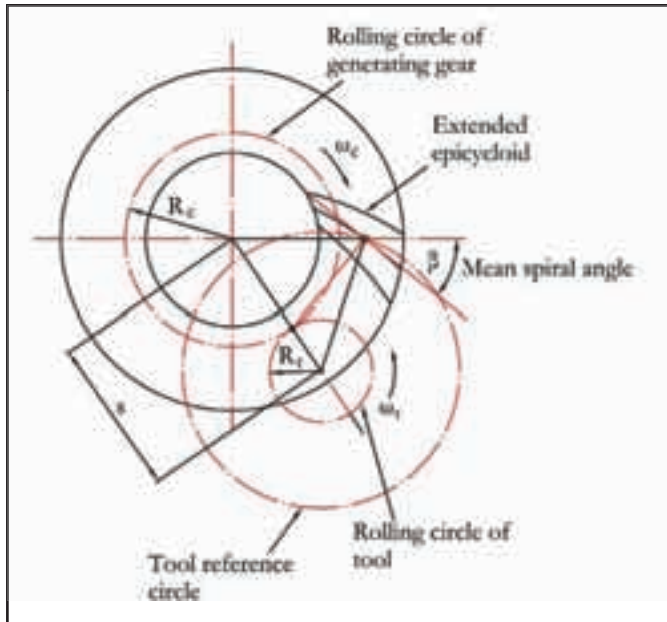


Figure 3—Generation of extended epicycloids.

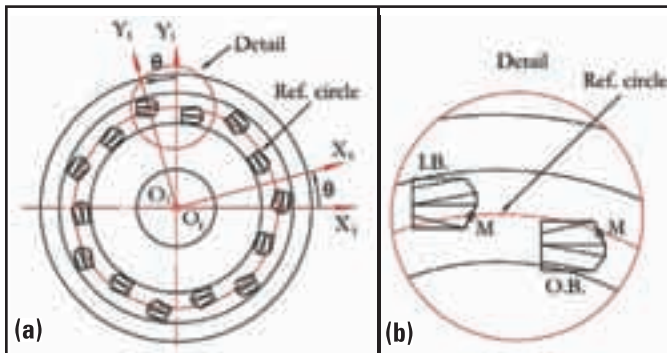


Figure 4—Face hobbing cutter head and blades.

$$\frac{\omega_w}{\omega_t} = \frac{N_t}{N_w} = R_w \quad (1)$$

Here, ω_t and ω_w denote the angular velocity of the tool and the work; N_t and N_w denote the number of blade groups and the number of teeth in the work, respectively. This related motion provides indexing between the tool and the work. The indexing relationship can also be represented by the rotation of the tool and the generating gear as,

$$\frac{\omega_c}{\omega_t} = \frac{N_t}{N_c} = R_{tc} \quad (2)$$

where ω_c and N_c denote the angular velocity of the generating gear and the tooth number of the generating gear, respectively. Meanwhile, the indexing motion between the tool and the generating gear kinematically forms the tooth surface of the generating gear with an extended epicycloid lengthwise tooth curve, as shown in Figure 3. The radii of the rolling circles of the generating gear and the tool are determined respectively by

$$R_c = \frac{N_c}{N_t + N_c} \cdot s \quad (3)$$

and

$$R_t = \frac{N_t}{N_t + N_c} \cdot s \quad (4)$$

here s is the machine radial setting.

The second set of related motions is the rotation of the generating gear and rotation of the work. Such a related motion is called rolling or generating motion and is represented as

$$\frac{\omega_w}{\omega_c} = \frac{N_c}{N_w} = R_a \quad (5)$$

where R_a is called the ratio of roll. Basically, the second set of related motions provides generated tooth geometry in the profile direction.

In the non-generating (Formate®) face hobbing process, only the first set of motion or indexing motion is provided for the gear tooth surface generation. Therefore, the gear tooth surfaces are actually the complementary copy of the generating tooth surfaces.

Tool Geometry

The Gleason face hobbing process uses TRI-AC® or PENTAC® face hobbing cutters. Face hobbing cutters are different from face milling cutters. The cutter heads accommodate blades in groups. Normally, each group of blades consists of an inside finishing blade and an outside finishing blade with reference point M located at a common reference circle, and the blades are evenly spaced on the cutter head (see Fig. 4). In some specially designed cutter heads, the inside and outside blades are not evenly spaced and therefore the blade radial position is correspondingly adjusted. Basically, the tool geometry can be defined by the major parameters of the blades and their installation on the cutter heads. Since the face hobbing tooth surfaces are kinematically generated by the cutting edges of the blades, an exact description of the cutting edge geometry in space is very important.

The blade edge geometry can be described in the coordinate system S_i that is connected to the cutter head with rotation parameter θ . The major parameters that affect the cutting edge geometry are: nominal blade pressure angle α , blade offset angle δ , rake angle λ , and effective hook angle κ .

Figure 5 shows a basic geometry of the inside and outside blade edges, which are represented in the coordinate system S_b that is fixed to the front face of the blade. The origin O_b coincides with reference point M at reference height h_b . Generally, the blade geometry consists of four sections: (a) tip, (b) Toprem®, (c) profile, and (d) Flankrem. Sections (a) and (d) are circular arcs with radii r_c and r_f respectively. Sections (b) and (c) can be straight lines, circular arcs, or other kinds of curves. Section (c) generates the major working part of a tooth surface. Toprem and Flankrem relieve tooth root and tip surfaces in order to avoid root profile interference and tooth tip edge contact. In order to obtain a continuous tooth surface, the four sections of the blade curves should be in tangency at connections. For a current cutting point P on the blade, the position vector and the unit tangent can be defined in the coordinate system S_b ,

$$\mathbf{r}_b = \mathbf{r}_b(u) \quad (6)$$

$$\mathbf{t}_b = \mathbf{t}_b(u) \quad (7)$$

where u is the parameter.

Equations 6 and 7 can be represented in the cutter head coordinate system S_i as

$$\mathbf{r}_i = \mathbf{M}_{ib}(\delta, \lambda, \kappa, R_b)\mathbf{r}_b(u) \quad (8)$$

$$\mathbf{t}_i = \mathbf{M}_{ib}(\delta, \lambda, \kappa, R_b)\mathbf{t}_b(u) \quad (9)$$

here matrix \mathbf{M}_{ib} denotes the coordinate transformation from S_b to S_i . Coordinate system S_i is used to represent the rotation of the cutter head with an angular displacement θ . From Figure 4, one can obtain the transformation matrix \mathbf{M}_{ii} and represent the blade geometry in system S_i as

$$\mathbf{r}_i = \mathbf{M}_{ii}(\theta)\mathbf{r}_i(u) = \mathbf{r}_i(u, \theta) \quad (10)$$

$$\mathbf{t}_i = \mathbf{M}_{ii}(\theta)\mathbf{t}_i(u) = \mathbf{t}_i(u, \theta) \quad (11)$$

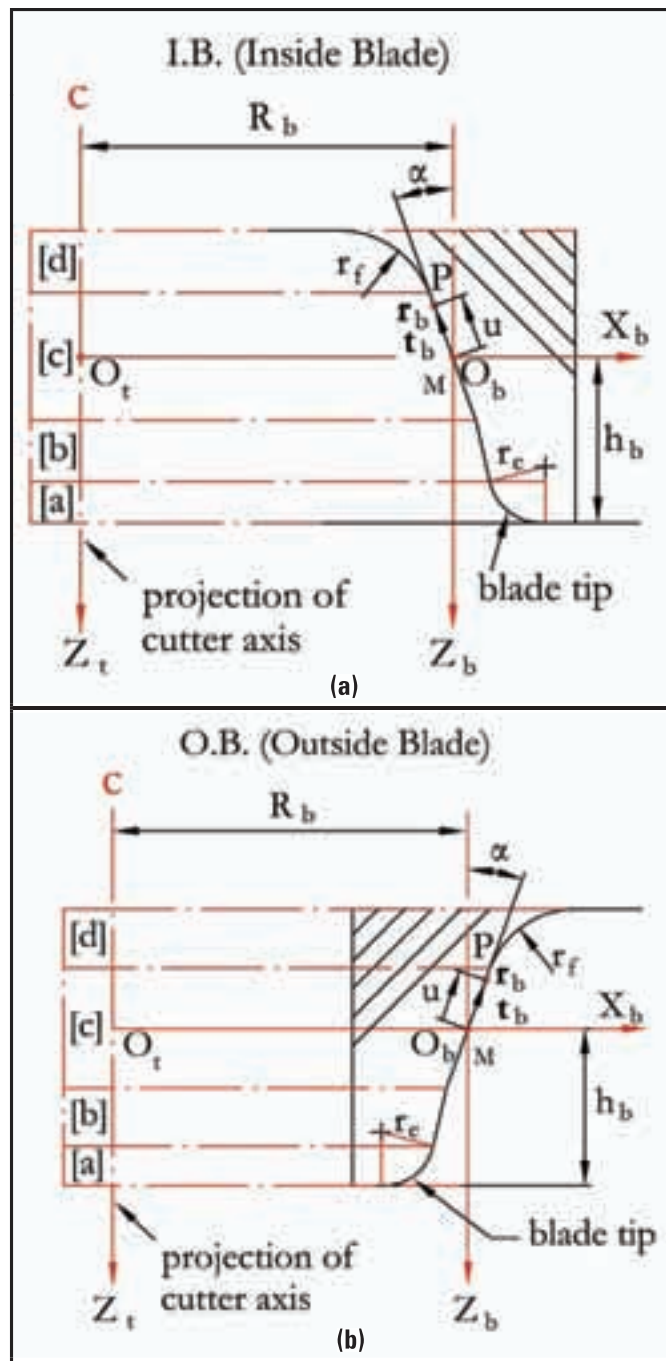


Figure 5—Blade geometry.

Kinematical Simulation of Face Hobbing Indexing Motion

As described above, the indexing motion generates the cutting path or the tooth lengthwise curves that are called the extended epicycloids (see Fig. 3). The indexing motion can be simulated and visualized in terms of the motion relationship between the generating gear and the cutter. Furthermore, such a motion can be represented in the cross-section plane that intersects the blade edges at the reference

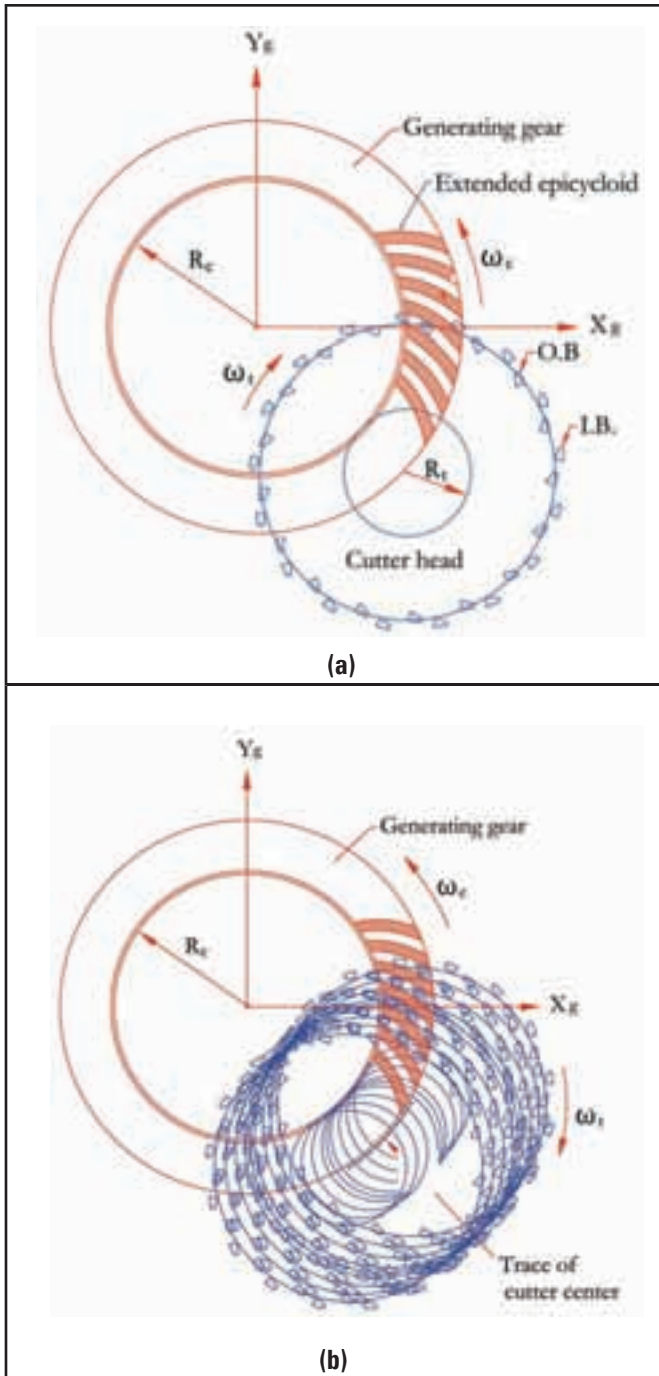


Figure 6—Simulation of face hobbing indexing motion.

$$\begin{bmatrix} x_g \\ y_g \end{bmatrix} = \begin{bmatrix} \cos[(1 + R_{tc})\theta] & -\sin[(1 + R_{tc})\theta] \\ \sin[(1 + R_{tc})\theta] & \cos[(1 + R_{tc})\theta] \end{bmatrix} \begin{bmatrix} x_t \\ y_t \end{bmatrix} + \begin{bmatrix} S_H \cos(R_{tc}\theta) + S_V \sin(R_{tc}\theta) \\ S_H \sin(R_{tc}\theta) - S_V \cos(R_{tc}\theta) \end{bmatrix}$$

Figure 7—Equation 12.

point M and is perpendicular to the axis of the generating gear so that the motion can be visualized on a plane, as shown in Figure 6. The simulation is based on the following matrix transformation, which represents the relative motion of the cutter head with respect to the generating gear.

(See Figure 7 for Equation 12)

The coordinate system S_g is connected to the generating gear (Fig. 6), and x_g and y_g are the coordinates of the tooth lengthwise curves, i.e., the extended epicycloids. Coordinates x_t and y_t specify points on the blades in system S_t . S_H and S_V are the initial horizontal and vertical settings of the cutter head. Giving a value to parameter θ corresponds to a specific cutting position. Figures 6 (a) and (b) respectively show a single cutting position and multiple cutting positions, from which the kinematical generation of tooth lengthwise curves and the tooth slots can be visualized.

Modeling of Face Hobbing Tooth Surface Generation

The face hobbing process can be implemented on the Gleason Phoenix® series CNC hypoid machines (see Fig. 8).

The machine tool settings and the tooth surface generation model can be derived based on traditional cradle-style mechanical machines. Computer codes have been developed to “translate” the machine settings, and CNC hypoid gear generators move together in a numerically controlled relationship with changes in displacements, velocities, and accelerations to implement the prescribed motions and produce the target tooth surface geometry.

In this paper, a generalized face hobbing kinematical model is developed. The proposed model, shown in Figure 9, is based on the mechanical spiral bevel and hypoid gear generators. The model consists of eleven motion elements, which are listed in Table 1. The cradle-style represents the generating gear, which provides generating roll motion between the generating gear and the generated work. In the non-generated (Formate®) process, the cradle is held stationary.

Face hobbing machine settings are: (1) ratio of roll R_a ; (2) sliding base X_b ; (3) radial setting s ; (4) offset E_m ; (5) work head setting X_p ; (6) root angle γ_m ; (7) swivel j ; and (8) tool tilt i . Although the kinematical model in Figure 9 is based on the cradle-style genera-

tors, considering the universal motion ability of CNC machines, the machine settings can be generally represented as

$$R_a = R_{a0} + R_{ac}(\varphi) \quad (13)$$

$$X_b = X_{b0} + X_{bc}(\varphi) \quad (14)$$

$$s = s_0 + s_c(\varphi) \quad (15)$$

$$E_m = E_{m0} + E_{mc}(\varphi) \quad (16)$$

$$X_p = X_{p0} + X_{pc}(\varphi) \quad (17)$$

$$\gamma_m = \gamma_{m0} + \gamma_{mc}(\varphi) \quad (18)$$

$$j = j_0 + j_c(\varphi) \quad (19)$$

$$i = i_0 + i_c(\varphi) \quad (20)$$

The first terms in Equations 13–20 represent the basic constant machine settings and the second terms represent the dynamic changes of machine setting elements, which might be kinematically dependent upon the motion parameters of the cradle rotation angle φ . In current practice, higher order polynomials are used (Ref.2). These motions can be realized through computer codes on the CNC machine. Equations 13–20 provide strong flexibility for generating all kinds of comprehensively crowned and corrected bevel gear tooth surfaces.

Matrix Representation of Motion Elements

In order to mathematically describe the generation process, the relative motions of the machine elements and their relationship have to be represented by a series of coordinate transformations established and rigidly connected to each motion element listed in Table 1. In current practice, higher polynomials are used (Ref. 2). System S_m is fixed to the machine frame 1 and is con-



Figure 8—Gleason Phoenix® II 275HC hypoid gear generator.

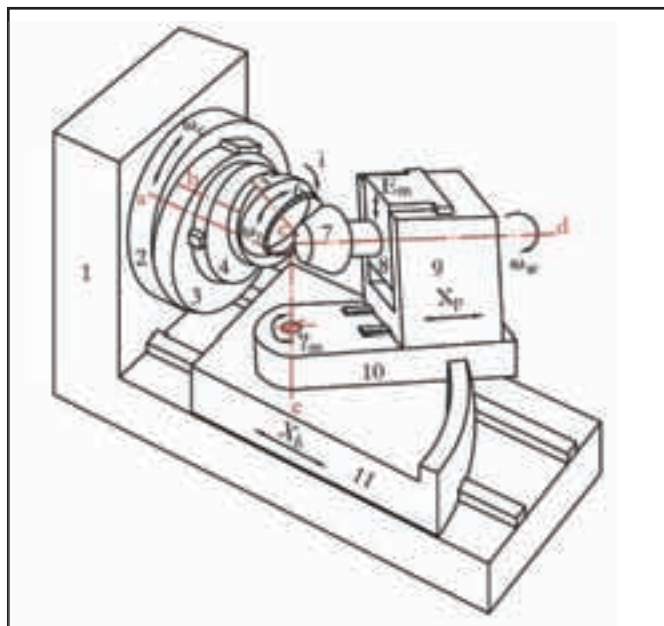


Figure 9—A kinematic model of mechanical hypoid gear generators.

Table 1—Machine Motion Elements and Axes of Rotation.	
Number of motion elements	Names of elements and related motion
1	Machine frame, motion reference
2	Cradle, rotation/cradle angle
3	Eccentric, radial setting
4	Swivel, swivel setting
5	Tilt mechanism, tilt setting
6	Tool cutter/head, rotation
7	Work, rotation
8	Work support, offset setting
9	Work head setting
10	Root angle setting
11	Sliding base setting
a	Cradle axis
b	Eccentric axis
c	Cutter head/tool spindle axis
d	Work spindle axis
e	Swivel pivot axis for root angle setting

$$\mathbf{M}_{wi} = \mathbf{M}_{wo}(\psi)\mathbf{M}_{op}(E_m)\mathbf{M}_{pr}(X_p)\mathbf{M}_{rs}(\gamma_m)\mathbf{M}_{sm}(X_b)\mathbf{M}_{mc}(\varphi)\mathbf{M}_{ce}(s)\mathbf{M}_{ej}(j)\mathbf{M}_{ji}(i)$$

Figure 10—Equation 23.

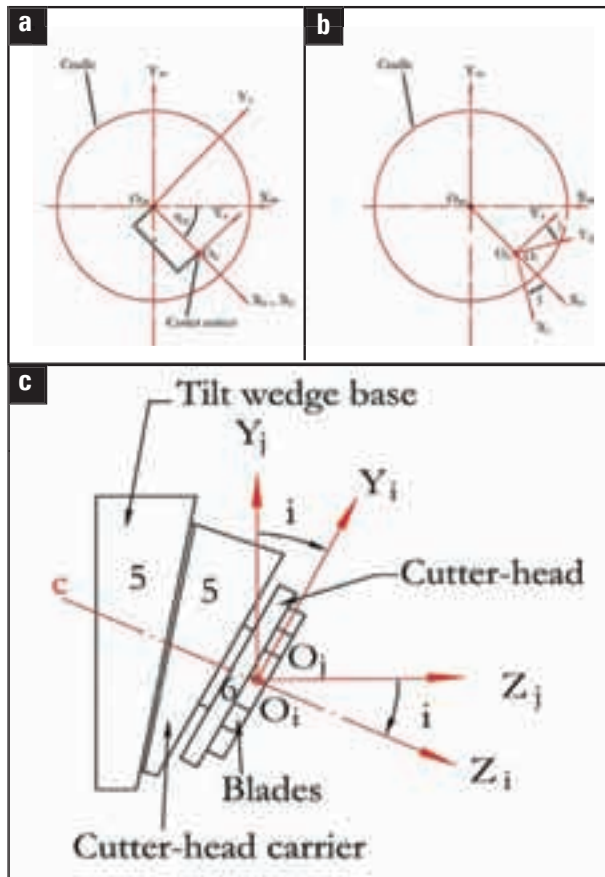


Figure 11—Relationships of coordinate systems S_m , S_e , S_i and S_w .

considered as the reference of the related motions. System S_s is connected to the sliding base element 11 and represents its translating motion. System S_r is connected to the root angle setting element 10 and represents the machine root angle setting. System S_c is connected to the cradle and represents the cradle rotation with parameter φ . System S_p is connected to the work head sliding setting element 9 and represents the work head setting motion. System S_o is connected to the work head offset setting sliding element 8 and represents the work head offset setting motion. System S_w is connected to the work 7 and represents the work rotation with angular parameter ψ . System S_e is connected to the eccentric setting element and represents the radial setting of the cutter head (see Fig. 11 (a)). System S_j is connected to the tilt wedge base element 5, which performs rotation relative to the eccentric element to set the swivel angle j (see Fig. 11 (b)). System S_i is connected to the cutter head carrier, which performs rotation relative to the tilt wedge base element to set the tool tilt angle i (see Fig. 11 (c)).

During tooth surface generation, at each cutting instant, a point on the blade edge generates a corresponding point on the work tooth surface. Through the coordinate transformation from S_i to S_w , the current cutting point P can be represented in the coordinate system S_w , namely,

$$\mathbf{r}_w = \mathbf{M}_{wi}(\theta, \varphi, \psi)\mathbf{r}_i(u, \theta) \quad (21)$$

$$\mathbf{t}_w = \mathbf{M}_{wi}(\theta, \varphi, \psi)\mathbf{t}_i(u, \theta) \quad (22)$$

where $\mathbf{M}_{wi}(\theta, \varphi, \psi)$ is a resultant coordinate transformation matrix with three parameters and is formulated by the multiplication of the following matrices representing the sequential coordinate transformations from S_i to S_w ,

(see Fig. 10 for equation 23)

where matrices \mathbf{M}_{wo} , \mathbf{M}_{op} , \mathbf{M}_{pr} , \mathbf{M}_{rs} , \mathbf{M}_{sm} , \mathbf{M}_{mc} , \mathbf{M}_{ce} , \mathbf{M}_{ej} and \mathbf{M}_{ji} can be obtained directly from Figures 12 and 13 and Equations 21 and 22 can be simply re-written as

$$\mathbf{r}_w = \mathbf{r}_w(u, \theta, \varphi) \quad (24)$$

$$\mathbf{t}_w = \mathbf{t}_w(u, \theta, \varphi) \quad (25)$$

here subscript “w” denotes that the vectors are represented in the coordinate system S_w .

Tooth Surface of a Non-Generated (Formate) Member

As discussed above, the non-generated (Formate) gear tooth surface is the complementary copy of the generating gear tooth surface, which is kinematically formed as the cutting path of the blade edge along an extended epicycloid lengthwise curve. In Formate gear generation, the cradle is held stationary and parameter φ is assumed to be zero. Therefore, Equations 24 and 25 can be re-written as

$$\mathbf{r}_w = \mathbf{r}_w(u, \theta) \quad (26)$$

$$\mathbf{t}_w = \mathbf{t}_w(u, \theta) \quad (27)$$

which give the position vector and a unit tangent at the current cutting point P on the gear tooth surface. The unit normal of the gear tooth surface can be derived as

$$\mathbf{n}_w = \mathbf{k}_w \times \mathbf{t}_w = \mathbf{n}_w(u, \theta) \quad (28)$$

where

$$\mathbf{k}_w = \frac{\partial \mathbf{r}_w}{\partial \theta} \quad (29)$$

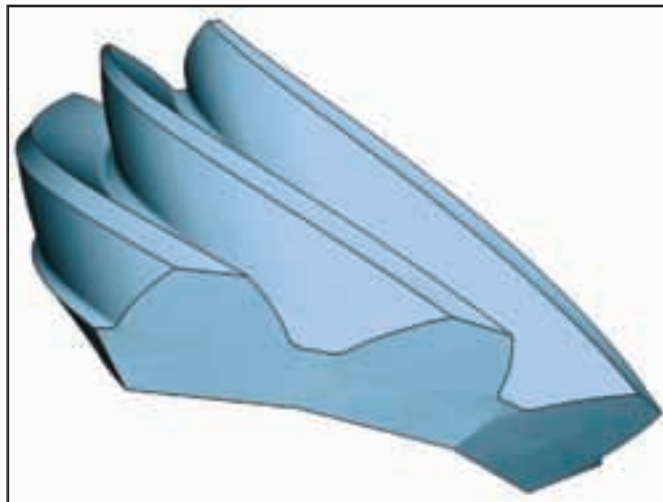
which represents the unit vector of hobbing speed. Equations 26–29 provide equations of position vector, unit tangent, and unit normal of a non-generated gear tooth surface.

Tooth Surface of a Generated Member

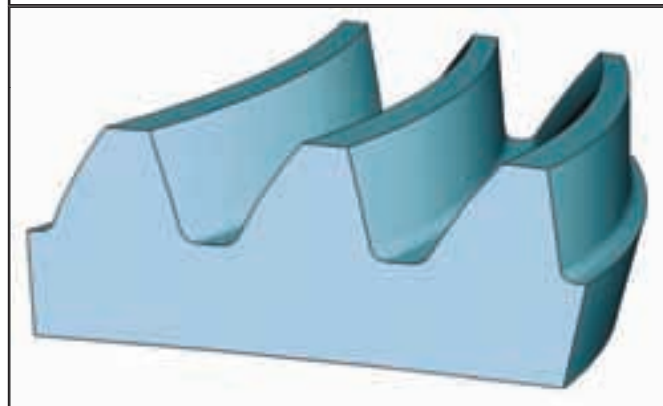
In addition to the relative hobbing motion or the indexing motion for a generated member, either gear or pinion, generating roll motion is provided and the generated tooth surface is the envelope of the family of the generating surface. The generated tooth surface can be represented as

$$\begin{cases} \mathbf{r}_w = \mathbf{r}_w(u, \theta, \varphi) \\ \mathbf{t}_w = \mathbf{t}_w(u, \theta, \varphi) \\ \mathbf{n}_w = \mathbf{n}_w(u, \theta, \varphi) \\ f_w(u, \theta, \varphi) = \mathbf{n}_w \cdot \mathbf{v}_w = 0 \end{cases} \quad (30)$$

where \mathbf{n}_w is obtained from Equation 28,



(a) Pinion tooth surfaces



(b) Gear tooth surfaces

Figure 12—Pinion and gear tooth surfaces of a face-hobbed hypoid gear drive.

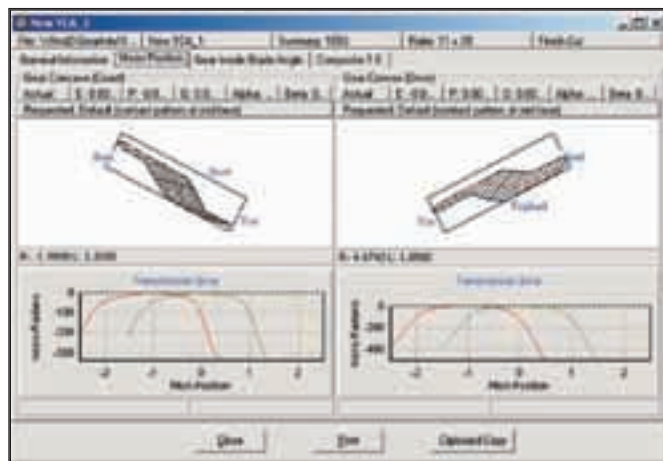


Figure 13—A TCA output interface.


and the relative generating velocity v_w is determined by

$$\mathbf{v}_w = \frac{\partial \mathbf{r}_w}{\partial \varphi} \omega_c \quad (31)$$

Equation $f_w(u, \theta, \varphi) = \mathbf{n}_w \times \mathbf{v}_w = 0$ is called the equation of meshing (Ref. 4). Equation 30 defines the position vector, the unit normal, and the unit tangent at the current cutting point P on the generated work tooth surface. All these vectors are considered and represented in the coordinate system S_w that is connected to the work. A unit cradle angular velocity, i.e., $\omega_c = 1$ can be considered. The equation of meshing is applied for determination of generated tooth surfaces.

Implementation of the Mathematical Models

Figures 12 (a) and (b) show geometric models of a pinion and a gear generated based on Equations 26–30. A very important application of the developed mathematical models is the development of tooth contact analysis for the face hobbled spiral bevel and hypoid gears. Tooth contact analysis (TCA) is a computational approach for analyzing the nature and quality of the meshing contact in a pair of gears. The concept of TCA was originally introduced by Gleason Works in the early 1960s as a research tool and applied to spiral bevel and hypoid gears (Ref. 7). Today, TCA theory has been substantially enhanced and generalized and applied in advanced synthesis of face milled spiral bevel gears (Refs. 8, 9).

Based on the developed mathematical models for face hobbing generation of spiral bevel and hypoid gears, an advanced TCA program for the face hobbing process has been developed for both non-generated and generated spiral bevel and hypoid gear drives. The program incorporates simulation of meshing of the whole tooth surface contact including the Toprem and Flankrem contact. Tooth edge contact simulation is also developed and included in the program. Figure 13 shows an example of the output interface of the advanced TCA. Typically, a TCA output illustrates bearing contact patterns on both driving and coast sides of the tooth surfaces and the corresponding transmission errors. Information on the gear drive assembling adjustments is also provided. 

Conclusion

This paper presents the tooth surface generation theory of the face hobbing process. The kinematics of face hobbing indexing are described and simulated. A generalized spiral bevel and hypoid gear tooth surface generation model for the face hobbing process is developed with the related coordinate systems that are directly and visually associated with the physical motion elements of a bevel gear generator. The generation model covers both Gleason non-generated and generated methods of the face hobbing process. And, it can also be adapted for the face milling process. Based on the developed mathematical model, an advanced TCA is developed and integrated into Gleason CAGE™ for the Windows system, which has been released worldwide.

References

1. Krenzer, T.J. "Face-Milling or Face Hobbing," AGMA Technical Paper, 90 FTM 13, 1990.
2. Stadtfeld, H.J. *Advanced Bevel Gear Technology*, The Gleason Works, Edition 2000.
3. Pitts, L.S. and M.J. Boch. "Design and Development of Bevel and Hypoid Gears using the Face Hobbing Method," Cat. #4332, The Gleason Works, 1997.
4. Litvin, F.L. *Gear Geometry and Applied Theory*, Prentice Hall, 1994.
5. Baxter, M.L. "Effect of Misalignment on Tooth Action of Bevel and Hypoid Gears," ASME paper 61-MD-20, 1961.
6. Krenzer, T.J. "The Effect of the Cutter Radius on Spiral Bevel and Hypoid Tooth Contact Behavior," AGMA Paper No. 129.21, Washington, D. C., October 1976.
7. "Tooth Contact Analysis Formulas and Calculation Procedures," The Gleason Works Publication, SD 3115, April 1964.
8. Litvin, F.L., Q. Fan, A. Fuentes. and R.F. Handschuh. "Computerized Design, Generation, Simulation of Meshing and Contact of Face-Milled Formate-Cut Spiral Bevel Gears," NASA Report CR-2001-210894, ARL-CR-467, 2001.
9. Litvin, F.L. and Y. Zhang. "Local Synthesis and Tooth Contact Analysis of Face-Milled Spiral Bevel Gears," NASA Contractor Report 4342, 1991.